IEEE Access
Multidisciplinary ⋮ Rapid Review ⋮ Open Access Journal

Received June 29, 2021, accepted July 9, 2021, date of publication July 14, 2021, date of current version July 23, 2021.

Digital Object Identifier 10.1109/ACCESS.2021.3097246

Photovoltaic Water Pumping: Comparison Between Direct and Lithium Battery Solutions

S. ORTS-GRAU[1], P. GONZÁLEZ-ALTOZANO[2], FRANCISCO J. GIMENO-SALES[1], I. BALBASTRE-PERALTA[2], C. I. MARTÍNEZ MÁRQUEZ[1], M. GASQUE[3], AND S. SEGUI-CHILET[1]

[1]Instituto Interuniversitario de Investigación de Reconocimiento Molecular y Desarrollo Tecnológico (IDM), Universitat Politècnica de València, 46022 Valencia, Spain
[2]Departamento de Ingeniería Rural y Agroalimentaria (DIRA), Universitat Politècnica de València, 46022 Valencia, Spain
[3]Departamento de Física Aplicada, Universitat Politècnica de València, 46022 Valencia, Spain

Corresponding author: S. Segui-Chilet (ssegui@eln.upv.es)

This work was supported in part by the Universitat Politècnica de València (UPV-Program ADSIDEO-cooperation 2017-Project Characterization of sustainable systems for the pumping of water for human consumption in developing regions or refugee camps in Kenya through the implementation of isolated photovoltaic systems with new generation lithium-ion batteries), and in part by the International Organization for Migration under Contract entitled "Design, Assembly, Testing and Documenting Parameters of Solar and Ion-Lithium Energy Storage Equipment for Powering of Water Pumps under Laboratory Conditions" from the Bureau for Humanitarian Assistance-USAID.

ABSTRACT This work presents the conversion of a photovoltaic water pumping system (PVWPS) to its corresponding battery-based solution, while maintaining the components of the PVWPS facility and adding the power converter needed to manage the operation of a lithium-ion battery. A complete analysis of the direct PVWPS is performed based on the values obtained by the monitoring system developed for the installation. The efficiencies and performance ratios of the various elements of the facility are calculated, as well as other relevant factors (such as irradiance thresholds). The dependence of some variables on the solar resource is analyzed to model the system. A similar study is carried out in the battery-based solution and a comparative analysis of the two modes of operation is then performed to find which aspects could be improved in the battery-based solution to increase the pumping time and total daily pumped volume. The results presented demonstrate the benefits of including a battery (reduction in start/stop cycles and improved performance on cloudy days). Aspects that can be improved to make the battery-based solution more efficient and achieve better results are suggested.

INDEX TERMS Photovoltaic water pumping systems, lithium batteries, battery-based pumping, water pumping, stand-alone photovoltaic system, sustainable development goals.

I. INTRODUCTION

A large part of fossil fuel-based energy consumption in non-electrified developing countries is in traditional electric and diesel water pumping systems used for irrigation or supplying drinking water [1], [2]. Dependence on fossil fuel-based energy is an obstacle in rural or remote communities [3] while secure access to water acts as an enabler for food security and assists sustainable development. Some of the main problems related to existing energy solutions include the absence of an electrical power grid, high fuel costs, dependency on imports, expensive and regular maintenance, high cost of transporting fuel to remote locations, greenhouse gas emissions, noise pollution, risk of water contamination, and environmental pollution [4]. These problems have led to the use of renewable energies for water pumping applications, with solar photovoltaics identified as a reliable and sustainable solution in rural areas of the developing world with high levels of annual irradiation [5], [6]. Several challenges must be faced to maximize the energy utilization and efficiency of pumping systems for irrigation [7] and domestic use [8]. Studies in the literature focus on comparing water pumping solutions while detailing the new technologies developed for optimal sizing and system improvement, performance analysis, control strategies, and economic evaluation (see the comprehensive overview included in [9] and reviews by [10] or [11]). Many factors, including pumping application and the location or purpose of an installation, determine the selection

The associate editor coordinating the review of this manuscript and approving it for publication was N. Prabaharan.

of various system configurations and these are addressed below.

Direct photovoltaic water pumping systems (DPVWPS) have gone in recent years from being a promising solution to a reality in many developing countries [1], [10], [12], [13]. DPVWPS are of interest when water consumption matches the solar resource profile or where an elevated tank stores water for use when solar irradiance is low. The loss factors affecting the performance of direct solutions are reviewed and analyzed in [14], where solar tracking systems are proposed to avoid the use of batteries in semiarid countries when irrigation is preferred in the early morning and late afternoon to prevent water evaporation and excessive work fatigue.

Several examples of DPVWPS can be found in the literature. A 1.5 kW_{pk} photovoltaic (PV) field was directly connected to a 882 W permanent-magnet synchronous motor coupled to a centrifugal pump [15]. The maximum efficiency reported was approximately equal to 25 % for a static head of 0.6 m and equal to 12 % for a static head of 11 m. Results obtained for four DPVWPS were described in [16]. The peak power of the PV fields (P_{PV}) was 2.1 kW_{pk} in three of the facilities and 2.8 kW_{pk} in the fourth facility. The PV field was connected to a 3 kVA variable speed drive (VSD) that drove a 1.5 kW motor coupled to a centrifugal pump. A test of the system components was performed using a linear voltage source with a pumping head of 65 m. Values of VSD efficiency (η_{VSD}) ranged from 87 % (at VSD frequency of $f_{VSD} =$ 29 Hz) to 95 % (for f_{VSD} from 48 Hz to 57 Hz) while the efficiency of the direct solution (η_{DPVWPS}) ranged between 21 % (at $f_{VSD} = 57$ Hz) and a maximum value (η_{DPVWPS_max}) of 30 % (at $f_{VSD} = 40$ Hz). η_{DPVWPS_max} was obtained for an irradiance (GI) of 700 W/m^2 and the threshold irradiance (GI_{thre}) was 300 W/m^2. Global average efficiency of the system ($\eta_{overall\_DPVWPS}$) reported in [16] was around 1.6 % and varied from 1.2 to 3.2 %. This value included PV efficiency with an average value (η_{PV_AV}) in the range of 10 %.

Hybrid systems, in which renewable energies are integrated with fossil-fuel based generators and storage systems, represent a solution for the transition from current electrical generation systems to future renewable energy based systems [9], [17], [18]. Depending on the characteristics of the application, a hybrid solution may be a better and more economically viable option than grid connection [19]. A more profitable use of renewable energy generation can be achieved through a variety of storage techniques [20]. Energy storage technologies that are easily scalable and modular with long lives and low maintenance may be the most suitable options for distributed systems [21]–[23]. The results presented in [24] show that a PV/battery/diesel hybrid system is more efficient and reliable than other analyzed configurations: a PV plant with battery storage system and a diesel-only system.

The inclusion of other energy resources in PV water pumping systems (PVWPS) is recommended in facilities in which some of the following problems are present:

- Water storage tanks, or the equipment necessary to handle, move, and install tanks, are unavailable [5], [12].
- A tank-based solution is more expensive than its equivalent with a battery storage system (BSS) [25].
- Energy consumption does not match the PV production profile: the main use of the water pumping system (WPS) is in the early morning and late afternoon [14] or for night-time pumping applications [26], [27].
- Water needed during periods of low solar radiation and on cloudy days [26], [28].
- When the WPS must work at its rated nominal conditions, or must ensure power supply continuity and system autonomy [29].

Battery coupled PVWPS solutions are described in [10], [12]. There are some examples in the literature on WPS that include a PV plant with BSS. Operation of these schemes was modelized in [30] but only simulated results were reported. The system analyzed in [27] was used for urban water pressurized networks and the storage of energy in tanks and batteries was compared. The use of a BSS in stand-alone PV direct pumping irrigation systems was analyzed in [31], [32].

There are very few examples of PVWPS systems including BSS and the most relevant are highlighted below. The PVWPS facility described in [33] had a $P_{PV} = 612$ W_{pk} and a battery of 24 V and 400 Ah with a maximum depth of discharge (DOD) limited to 50 %. The facility included a storage tank of 500 L and a Shurflo 9300 submersible pump (24 V dc). The PVWPS facility presented in [34] had a maximum consumption of 60 Wh/day and included the following devices: a lead-acid battery with 12 V and 131 Ah; a 21 W_{pk} PV module; a pulse width modulation (PWM) charge regulator; and a 60 W pump. A 12.65 kW_{pk} PV field and a 168 V/210 Ah lead-acid battery were applied for the irrigation of a tomato farm in Tunisia, obtaining a performance ratio for the PVWPS system equal to 21.1 % [29].

A comparative performance analysis between several WPS and including various storage solutions was made in [35], where a DPVWPS was compared with schemes that included lead-acid batteries, supercapacitors, and a hybrid solution combining battery and supercapacitors. An experimental study was performed using a 20 W_{pk} PV module, a 24 Wh battery (12 V and 2 Ah), a 4.2 Wh and 12 V supercapacitor bank, as well as a 12 V and 14.4 W dc motor. Total dynamic heads (TDH) of 2 and 3 m were compared, and efficiencies were obtained for the systems of between 2 % for $TDH =$ 3 m with the direct solution and 23 % for $TDH = 2$ m and a supercapacitor. The efficiency of the system with battery storage was 8−14 % for $TDH = 2$ m and 2−16 % for $TDH =$ 3 m. The authors concluded that the battery storage configuration showed, on average, better results than the supercapacitor configuration. Althoug supercapacitors have a longer lifespan and are more reliable, the high cost of the solution made it unfeasible. Some of the problems reported by the authors in

relation to lead-acid batteries (lifetime of just a few years and poor temperature performance) are now overcome thanks to lithium-ion batteries (LIB).

A comparison between a direct solution and its corresponding battery-based solution was made in [28]. The facility used a 110 W_{pk} PV module with 35 V and 3.15 A in the maximum power point or MPP, and a PWM charge controller that managed the charging and discharging processes of a 24 V and 100 Ah gel lead-acid battery in the PVWPS + BSS scheme. The dc load output of the PWM regulator was connected to a linear current booster, which in turn fed a Shurflo 9300 dc pump that operated with a nominal voltage of 24 V and demanded 120 W. The results show that efficiency in DPVWPS mode varied between 10 % to 20 % and efficiency values between 6 % to 11 % were obtained for the battery-based PVWPS mode for *TDH*s of 5 m and 9 m respectively. Values for system efficiencies (including the PV module efficiencies) were also presented.

Among the different chemistries available for batteries [36], [37], LIB storage has experienced the greatest development in recent years and its characteristics and applications are described in [38]. Until the commercial availability of LIB storage solutions, batteries in PVWPS were considered a source of weakness due to a lack of reliability and short life span [7]. They were little used because of their high purchase and replacement costs [5], the dependence of their performance on the climatic conditions of the installation, periodic maintenance, and the difficulty of expanding capacity by adding new units in parallel. LIBs are currently replacing lead-acid batteries in grid-connected and stand-alone PV systems. The greater initial cost of an LIB solution is compensated by the longer lifespan and improved operating conditions (such as voltage stability and greater DOD). There are studies on LIB aging [39] and the accurate evaluation of battery cell inconsistency [40] that are important when considering a second life for electric vehicle LIBs in PV systems. When capacity drops below 80 % of original capacity, their subsequent use in PV systems could reduce the cost of these facilities [41].

This paper is within the framework of an R&D line that has already resulted in a previous study [42] on a PVWPS with a lithium-ion battery (PVWPS + LIB). In this previous study, the PV monitoring system developed for the PVWPS + LIB facility was described in detail. Additionally, some preliminary experimental results of the WPS facility were presented. The project concept started with a request from the International Global Solar Energy & Water Advisor at the International Organization for Migration (IOM) who has extensive experience in the use of WPS in humanitarian and development projects [4]. The project is also aligned with the Sustainable Development Goals set out by the United Nations 2030 Agenda [43].

In this new contribution, the authors analyze in depth the direct PV pumping system based on the measurements acquired with the monitoring system. Efficiencies and performance ratios (*PR*) are obtained from the powers and energies in different parts of the system. The evolution of several variables and their dependence on the solar resource are analyzed to model the system response. A battery-based solution is then proposed that adds only the necessary components to manage the charging and discharging of the battery from the PV field. The values obtained with the battery-based solution are compared with those obtained with direct solution, using days with a similar irradiance profile in the comparison. The results make it possible to propose modifications to the system. The main problems found related with the equipment used in the experimental work are detailed.

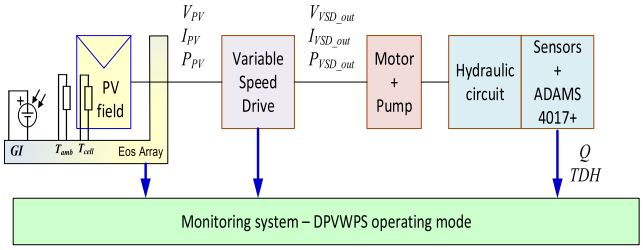

FIGURE 1. Block diagram of the direct solution and the main measured magnitudes.

The remainder of the article is organized as follows. Section II summarizes the main features of the DPVWPS facility and presents the key values of this operating mode (such as efficiencies and performance ratios). Section III justifies the use of batteries in PVWPS and highlights lithium-ion batteries. Section IV details operation in PVWPS + LIB mode and presents the values of the main estimated parameters. Section V develops a comparison of both operating modes (direct vs battery-based) and determines which aspects can be improved in the battery-based solution. Finally, the findings on the main contributions of this work are presented.

II. DESIGN AND CHARACTERIZATION OF THE DIRECT PV WATER PUMPING FACILITY

The main parts of a DPVWPS facility, and the monitoring system, are described in [42]. FIGURE 1 shows a block diagram of the DPVWPS and details the main magnitudes that are acquired for the study. The rated power of the submersible motor-pump group (P_{mp}) is 1.5 kW and it is driven by a 2.2 kW VSD that generates a 200 V three-phase system with a variable frequency f_{VSD} that enables controlling the operation point of the motor-pump group (i.e., its power consumption). The VSD enables connecting a PV field and a single-phase ac system. In the DPVWPS mode of operation the PV field is connected to the dc input of the VSD. The VSD includes a maximum power point tracking (MPPT) algorithm that extracts the maximum power and energy from the PV array and matches P_{PV} with P_{mp} for a wide range of operating conditions. The main characteristics of the PV module (in standard test conditions or STC) and the VSD are detailed in Table 1.

TABLE 1. PV module and VSD characteristics.

V_{OC} = 45.35 V	V_{MPP} = 36.71 V	P_{MPP} = 305 W_{pk}
I_{SC} = 8.79 A	I_{MPP} = 8.31 A	NOCT = 45±2 ºC
$\beta_{V_{OC}}$ = –0.34 %/K		$\beta_{V_{MPP}}$ = –0.4 %/K
$\alpha_{I_{SC}}$ = +0.06 %/K		$\gamma_{P_{MPP}}$ = –0.45 %/K
$V_{VSD\,max}$ = 400 V		$V_{VSD\,min}$ = 180 V
$V_{VSD\,MPP}$ = 280 – 330 V		

The maximum number of PV modules that can be connected in series in the PV field is obtained in (1) when considering the maximum VSD input voltage ($V_{VSD\,max}$) and the open circuit voltage (V_{OC}) of the PV module in STC:

$$N_{MS_{max}} \leq \frac{V_{VSD_{max}}}{V_{OC_{STC}}} = \frac{400}{45.35} = 8.8 \tag{1}$$

The PV field has eight modules connected in series with a P_{PV} equal to 2.44 kW_{pk} and a V_{MPP_STC} of 293.6 V, and which is in the range of the MPP of the VSD detailed in Table 1. The oversizing of P_{PV} with respect to the motor-pump group power (P_{mp}) is equal to 1.6 and is within the typical values in DPVWPS (between 1.4 and 1.9). Voltage values in winter are near STC values and a significant decrease in voltage and power occurs in summer due to high ambient temperatures. For midday in central summer (1000 W/m^2 and T_{amb} = 30 °C) the values of PV cell temperature (T_{cell}), MPP voltage (V_{MPP}), and MPP power (P_{MPP}) can be calculated as follows:

$$T_{cell} = T_{amb} + (NOCT - 20) \cdot \frac{E}{800} \tag{2}$$

$$V_{MPP} = V_{MPP_{STC}} \cdot \left(1 + \frac{\beta}{100} \cdot (T_{cell} - 25)\right) \tag{3}$$

$$P_{MPP} = P_{MPP_{STC}} \cdot \left(1 + \frac{\gamma}{100} \cdot (T_{cell} - 25)\right) \tag{4}$$

By substituting the corresponding values from Table 1 in (2), (3), and (4), and considering the number of PV modules in series, the values obtained are T_{cell} = 61.25 °C, V_{MPP} = 251 V, and P_{MPP} = 2042 W.

A total of 47 days of operation in the DPVWPS mode with different levels of irradiation were analyzed. The following plots describe the operation of the direct solution and represent the average values of different magnitudes in one-minute recording intervals (t_k = 1 minute) on October 2 and 3. Table 2 shows the values of the main parameters obtained for these two days together with the average values obtained for a set of 27 days with operation in direct mode. These 27 days were selected among the total of 47 days because the average peak sun hours value they show (PSH_{AV} = 5.26) is the same as that obtained with the set of 15 days used to analyze the PVWPS + LIB behavior in Section IV. Thus, the average values of the key magnitudes estimated with the two operating modes can be compared.

FIGURE 2-a shows irradiance (GI, in W/m^2), P_{PV}, power in the output of the VSD (P_{VSD_out}), and hydraulic power (P_h) from 08:00 to 20:00 on October 2 and 3 (10/2 and 10/3).

TABLE 2. Values obtained for the direct solution on October 2 and 3 and average values considering 27 days.

	10/2	10/3	$AV_{27\ days}$
PSH	2.01	6.54	5.26
TDH_{AV} (m)	18.64	21.49	20.45
V_d (m^3/d)	10.12	70.32	55.34
E_{PV} (kWh/d)	2.02	14.96	11.37
PR_{PV} (%)	41.21	93.81	88.10
E_{VSD_out} (kWh/d)	1.62	11.87	9.24
PR_{VSD} (%)	84.54	79.35	81.52
E_h (kWh/d)	0.53	4.18	3.19
PR_{mp} (%)	32.93	35.23	34.31
PR_{DPVWPS} (%)	26.43	27.96	27.95
PR_{syst} (%)	1.71	4.12	3.87
f_{VSD_AV} (Hz)	32.39	44.50	41.61
η_{VSD_max} (%)	98.79	96.72	97.94
η_{VSD_AV} (%)	84.38	81.28	83.02
η_{mp_max} (%)	36.79	36.26	36.47
η_{mp_AV} (%)	31.38	35.02	33.47
η_{DPVWPS_max} (%)	30.85	30.92	30.79
η_{DPVWPS_AV} (%)	26.53	28.40	27.82
Pumping time (min)	129 (2h:09min)	543 (9h:03min)	456.37 (7h:36min)
Start/stop cycles	10	1	4.85

The three power values, expressed in watts, refer to the left axis and the differences between the curves correspond to the power losses in the DPVWPS components: power losses in the VSD ($PL_{VSD} = P_{PV} - P_{VSD\_out}$) and losses in the motor-pump group ($PL_{mp} = P_{VSD\_out} - P_h$). The GI profile during 10/2 corresponds to a cloudy day while the 10/3 profile corresponds to a sunny day with 2.01 and 6.54 PSH respectively (as detailed in Table 2). The GI start-pumping threshold on 10/3 (GI_{thre_start}) is equal to 300 W/m^2, while the pumping stop (GI_{thre_stop}) is at 200 W/m^2 (FIGURE 2-a). These results are consistent with those obtained during seven completely sunny days operating in DPWPS mode, and during which the average and standard deviation values (301.30 ± 12.30) W/m^2 and (208.90 ± 10.10) W/m^2 were obtained for GI_{thre_start} and GI_{thre_stop} respectively.

The values of Q and total dynamic head (TDH) are shown in FIGURE 2-b. Maximum flow rate (Q_{max}) is equal to 2.54 L/s, when f_{VSD} is around 50 Hz. The TDH is the sum of the discharge head, the static water level, the drawdown distance, and the distance equivalent of the water friction in the pipe [8], [10], [11]. Drawdown and friction losses are both dependent on the pumping rate, so TDH always shows a dependence on Q, as can be seen in the TDH plot during pumping time and the small step at the start and stop of pumping. Average TDH (TDH_{AV}) during 10/3 is 21.49 m, with a maximum of 23.25 m at midday and a static discharge head of 15.94 m (when Q = 0 L/s). The total daily volume (V_d) during 10/2 and 10/3 is 10.12 m^3 and 70.32 m^3 respectively (Table 2).

A linear relationship between V_d and PSH was found in DPVWPS mode (FIGURE 3), and as discussed later, when the system is operating in PVWPS + LIB mode, this relationship enables a reliable estimate of the volume that would

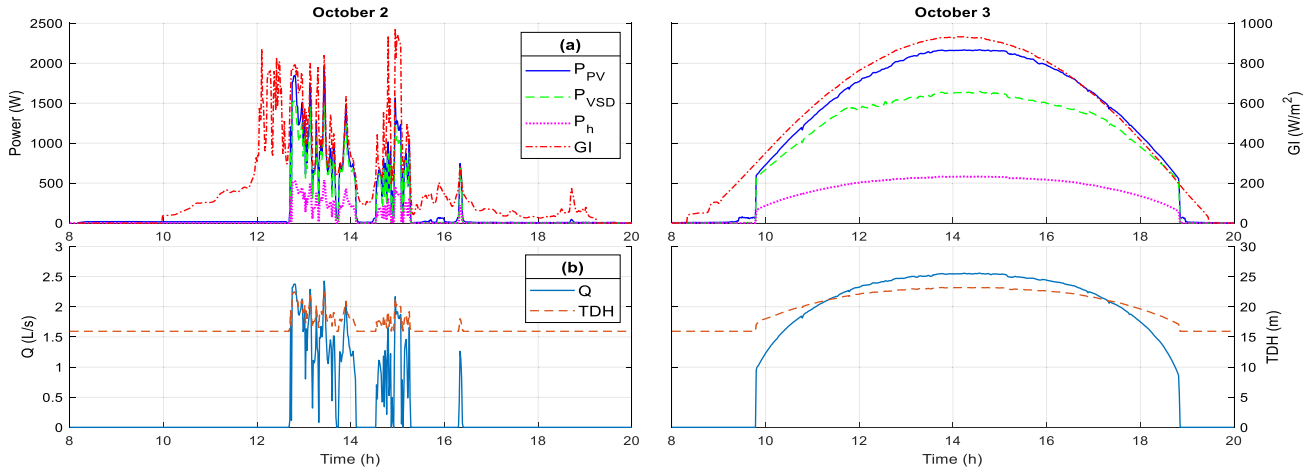

FIGURE 2. DPVWPS mode from 08:00 to 20:00 on October 2 and 3. (a): Values of powers (PV, VSD output, and hydraulic) and irradiance. (b): Evolution of flow and total dynamic head.

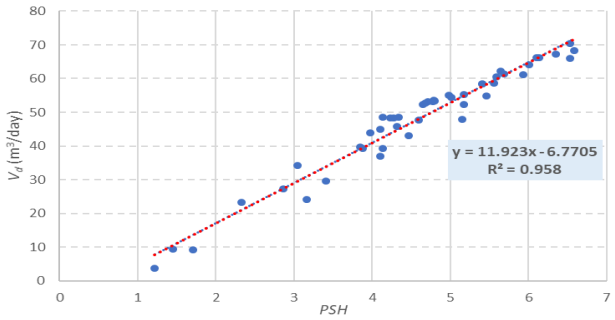

FIGURE 3. Relationship between daily volume and peak sun hours in 47 days of DPVWPS.

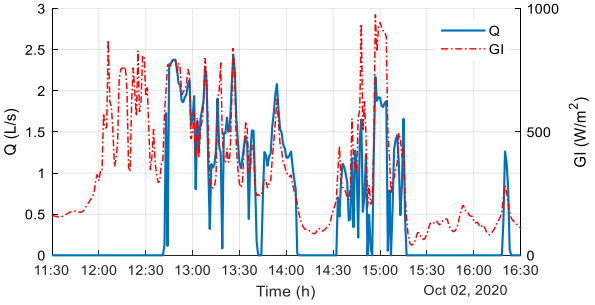

FIGURE 4. Values of flow and irradiance in the direct solution from 11:30 to 16:30 during 10/2.

be pumped with the direct solution. The average daily volume (V_{d_AV}) in the set of 27 days selected in DPVWPS mode is equal to 55.34 m^3.

The energy not generated in the direct solution when *GI* is lower than the irradiance pumping thresholds, or when P_{PV} exceeds the VSD rating, could be stored in an LIB for later use. As an example, at solar noon on 10/3 P_{PV} presents a flat plane located at 2160 W, while the *GI* curve presents a bell shape with a well-defined maximum value (around 935 W/m^2) (FIGURE 2-b). The flattening of the P_{PV} occurred because the nominal power value of the VSD was already reached, and therefore, the VSD controller adjusted the working point of the PV field to achieve a balance between generated and consumed power. During this interval, the PV field was no longer in the MPP, although it remained extremely close to that point as the PV field was designed for this DPVWPS operating mode. If the PV field had more peak power installed, there would be excess energy that could be used for other purposes, or stored in a battery for later use, thereby avoiding clipping energy losses.

For the data acquired on 10/2, the first aspect to highlight is the delay at $GI > GI_{thre\_start}$ (around 11:58) and at the start of pumping when flow rate is measured ($Q > 0$ L/s at 12:42 with $GI = 575$ W/m^2). This delay can be seen in the time interval between 11:30h and 16:30h on 10/2 shown in FIGURE 4 and is due to the VSD control which, on cloudy days, when *GI* levels are higher than GI_{thre_start}, introduces a delay in the pump start-up to avoid start/stop cycles. Despite the inclusion of this algorithm, up to ten start/stop cycles were counted. The failed start-up cycles are more noticeable in FIGURE 5 with low VSD efficiency values ($\eta_{VSD} < 15$ %) and in FIGURE 2-a with low P_{PV} values when $P_h = 0$ W. Frequent start/stop cycles cause mechanical damage to the pumps, reduce lifespan, and increase maintenance costs. These stops are usually between 2 to 15 minutes and are easily avoidable if the system includes a battery to keep the system pumping during these intervals.

The total efficiency of the system (η_{DPVWPS}) shown in FIGURE 5 is defined as P_h/P_{PV}, and so it excludes η_{PV}, which depends on PV technology and the quality of the PV cells used. As indicated in Table 2, the maximum efficiency of the system (η_{DPVWPS_max}) reaches 30.92 % on 10/3, with an average value (η_{DPVWPS_AV}) of 27.82 % in the set of 27 days selected for comparative analysis.

The variation in the VSD efficiency (η_{VSD}) and the motor-pump group (η_{mp}) on 10/3 (a sunny day) is greater during the beginning and end of the pumping interval, while η_{mp} presents a more constant and opposite trend (FIGURE 5).

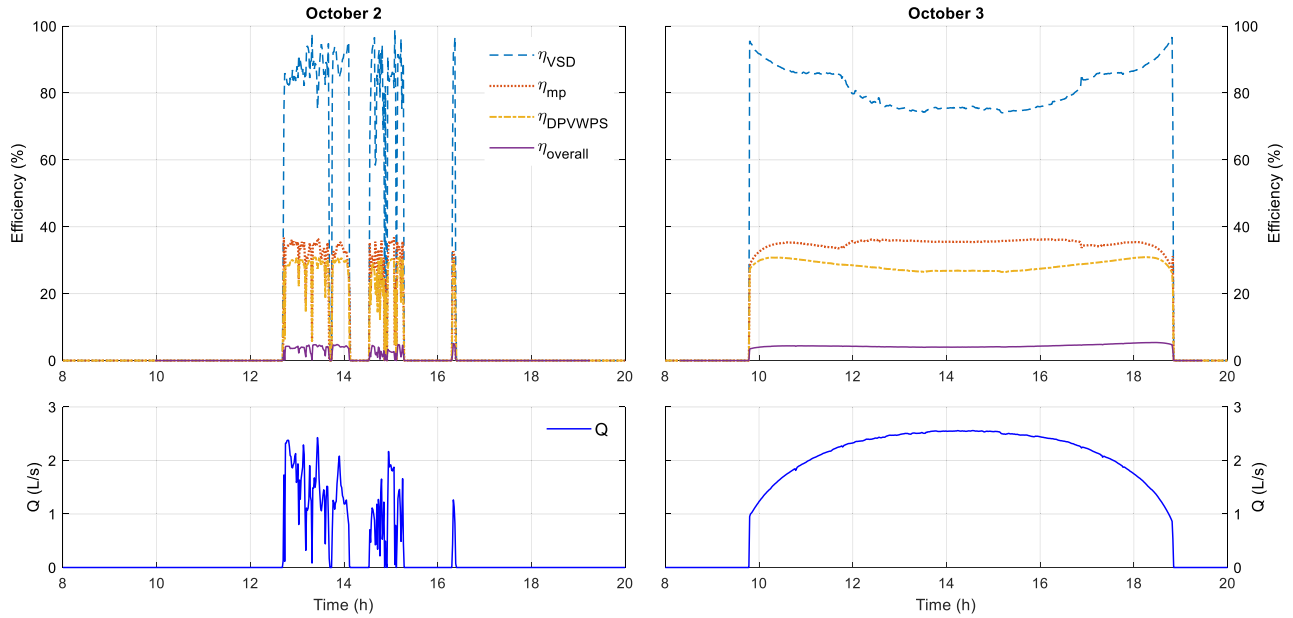

FIGURE 5. Values of efficiencies (VSD, motor-pump, DPVWPS, and overall system) and flow in the direct solution from 08:00 to 20:00 during October 2 and 3.

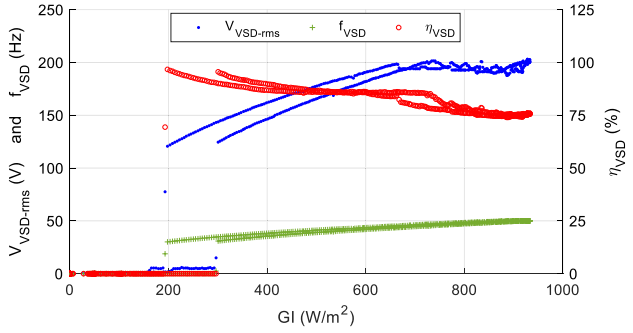

FIGURE 6. Rms voltage, frequency, and efficiency in the VSD against irradiance in the direct solution from 08:00 to 20:00 during 10/3.

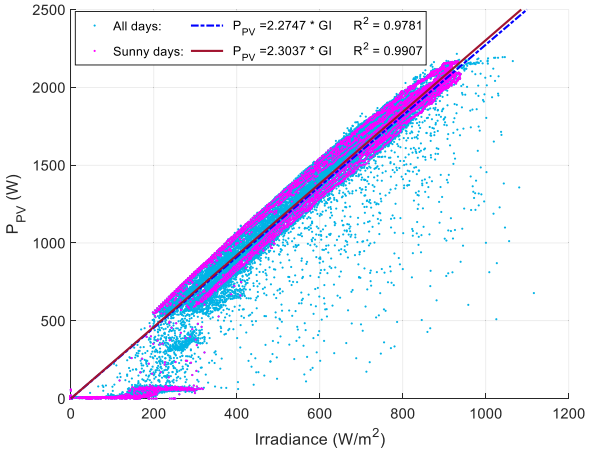

FIGURE 7. Fitting relationship between PV power and irradiance for 47 days of operation with different weather conditions (blue dots) and for 7 sunny days (purple dots) in the direct solution.

By discarding the beginning and end values of the η_{VSD} plot, two regions can be distinguished – with η_{VSD} around 85 % with low GI and values close to 75 % during the central hours. The opposite behavior is observed in η_{mp}, although the variations are smaller than those observed in η_{VSD}. Although Q_{max} is achieved at noon, when the motor-pump group is near to its rated operating conditions, the values obtained for η_{DPVWPS} at noon are the lowest in the operating interval.

During the pumping stage, the values of η_{DPVWPS} are between 30.7 % (beginning and end of the pumping interval) and 26.3 % (at approximately noon). It should be noted that the reduction in the η_{VSD} during midday penalizes η_{DPVWPS}, with a difference of 4.4 % during the pumping period.

The MPPT algorithm included in the VSD control adjusts the rms voltage (V_{VSD_rms}) and frequency (f_{VSD}) of the three-phase ac output to balance PV generation and motor-pump consumption. FIGURE 6 shows the dependence of V_{VSD_rms}, f_{VSD}, and η_{VSD} on GI during 10/3 with a smooth variation in GI throughout the day. The VSD operates near its rated values (200 V and 50 Hz) for GI above 800 W/m^2, corresponding with the minimum values of η_{VSD} in all the range of operation.

The PV energy potentially available can be estimated from GI values and the excess energy generated and not used that could be stored in a battery can then be determined. The linear relationship between the values of P_{PV} and GI obtained when the facility operates in DPVWPS mode during the 47 days of study with various solar coverages (blue dots in FIGURE 7) was performed and gave a fitting factor of $k_{GI\_all} = 2.2747$ ($R^2 = 0.978$). Moreover, a fitting coefficient $k_{GI\_sunny} = 2.3037$ ($R^2 = 0.990$) was obtained from a set of 7 sunny days with values of PSH ≥ 6, similar to 10/3 (purple dots in FIGURE 7).

Table 3 includes the PV energy estimates (E_{PV_est*}) obtained for October 2 and 3 and the average values obtained

TABLE 3. Estimation of the PV energy generated on October 2 and 3 and average values considering 27 days.

	10/2	10/3	$AV_{27\ days}$
E_{PV} (kWh/d)	2.02	14.96	11.37
$k_{GI1} = k_{GI\_all}$	2.2747	2.2747	2.2747
E_{PV_est1} (kWh/d)	4.57	14.87	11.70
ΔE_{PV_est1} (%)	226.22	99.37	104.69
k_{GI2}	2.40	2.40	2.3037
E_{PV_est2} (kWh/d)	4.82	15.69	11.85
ΔE_{PV_est2} (%)	245.18	105.21	106.02

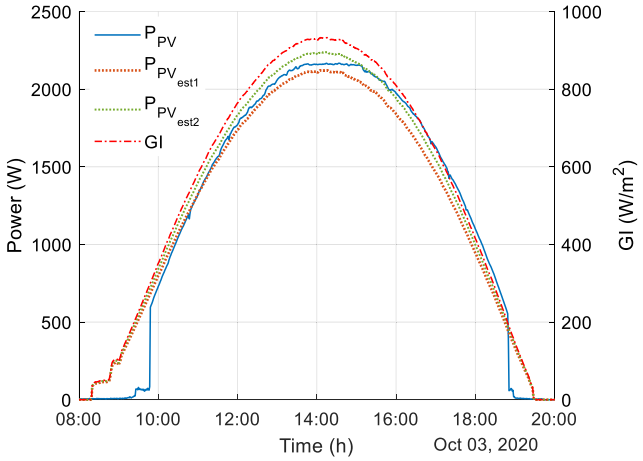

FIGURE 8. PV power, PV power estimations 1 and 2, and irradiance throughout the day in the direct solution from 08:00 to 20:00 during 10/3.

for the set of 27 days operating in DPVWPS mode. An initial assessment is made using the value of k_{GI_all}. This value, used on 10/3, produces an estimate of E_{PV} (14.87 kWh/day) that is close to the real value obtained (14.96 kWh/day). The evolution of P_{PV} on 10/3 can be compared with that of P_{PV_est1} in FIGURE 8, where a second P_{PV} estimation (plotted as P_{PV_est2}) is performed using $k_{GI2} = 2.4$. The E_{PV} gain (ΔE_{PV}) obtained on 10/2 (a cloudy day) is 220 % considering k_{GI1} and 245 % if k_{GI2} is used, confirming that a PVWPS + LIB system with MPPT tracking could make much better use of the PV resource on cloudy days.

Values shown in Table 3 suggest that an increase in the range of 4 % to 6 % in E_{PV} can be expected on average for this system. This improvement in E_{PV} should compensate for the added losses of the battery-based solution (LIB and power converter unit).

III. USE OF LITHIUM-ION BATTERIES IN PVWPS

As mentioned in the introduction, battery-based PVWPS are not the most common solution in remote locations, in which the use of an auxiliary generator avoids the use of batteries and ensures the supply of energy during cloudy periods. The main disadvantages of PVWPS with batteries are:

- Reduction in the efficiency of the overall system.
- The system will be more expensive and less reliable as more elements are included and will require additional maintenance: battery; charge regulator; power converter unit (PCU); etc.
- The use of PWM charge controllers establishes operating voltages below V_{MPP}, which significantly decreases P_{PV} compared to an MPPT charge controller, especially in places with high T_{amb}.
- Additional under- and over-charge protection circuitry is needed that adds cost and complexity to the system.

The main advantages of PVWPS with batteries are:

- Improved coupling between the PV generator and the motor-pump group, with a PV generator operating in the MPP for a wide range of irradiance levels.
- The current required for start-up and normal operation of the motor can be supplied continuously.
- The pump will operate longer, and so a less powerful pumping system will be required for the same needs.
- The installation can use a booster pump to create water pressure during low irradiance periods.
- The system prevents pump stop/start cycles caused by the passage of clouds.

Although lead-acid batteries dominated the market for both grid-connected and off-grid PV systems until approximately 2018, LIBs have prevailed in the market for grid-connected systems from 2016 onwards [44], [45] and are also used in off-grid systems. Existing energy storage systems were presented in [20], [37], and a comparison made between the various battery chemistries available in the market, as well as an analysis of their performances, was included in [46], [47]. The LIB technology used in PV systems is the same as electric cars, hybrid cars, or in power network management systems [48], [49]. Therefore, technological advances in the field of energy storage, mainly in the electric vehicle industry, have facilitated the development of LIB with more than 6800 life cycles (more than 18 years with one charge and discharge process per day).

Regarding [20], [50], LIBs offer many advantages compared to other lead batteries: they are almost 100% effective in charging and discharging processes; have longer lives; offer constant capacities (less dependent on discharge current); offer higher power densities; reduced maintenance; more stable voltages during discharge cycles; enable connections up to hundreds of volts and thousands of watt-hours; and are environmentally safer. LIBs are becoming a cost-effective, reliable, and high-performance solution in a wide range of applications and including power generation in isolated locations not connected to conventional power grids [49]. Given the expected increase in the use of this storage technology, the life cycle assessment of lithium-ion batteries is a topic of great interest today, where the most sustainable solutions must be correctly identified and supported [20].

The use of PV systems combined with battery energy storage can boost energy sustainability in remote locations, reduce greenhouse gas emissions and on-site pollution, eliminate dependence on fossil fuels, and reduce the cost of energy [10]. Large oversizing factors for the PV field and

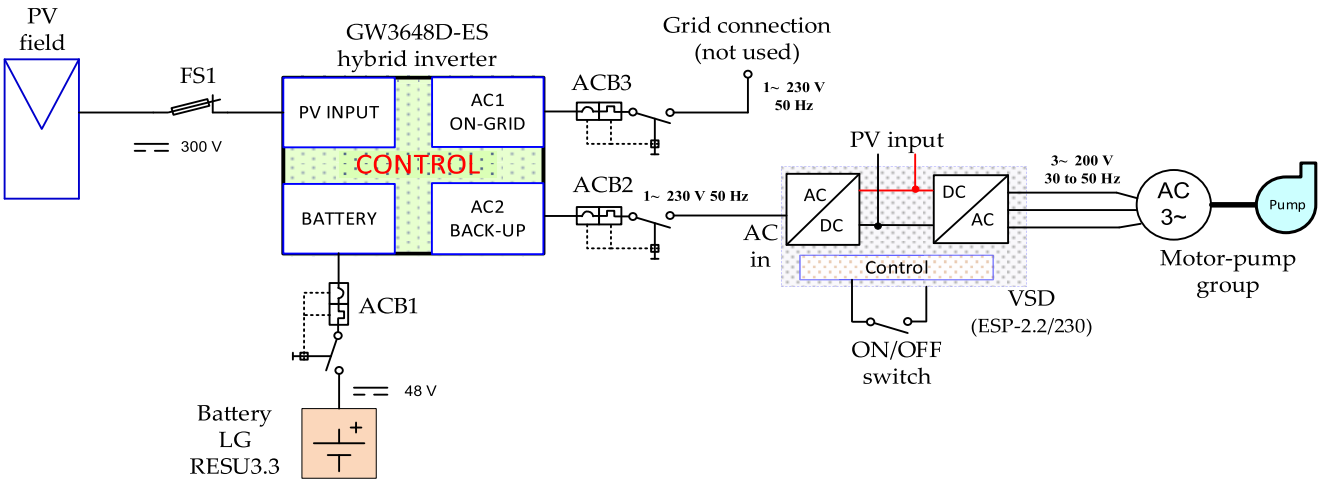

FIGURE 9. Block diagram of the battery-based solution with voltage conditions in the various parts of the system.

high-capacity batteries minimize the use of auxiliary generators and reduce the need for a continuous supply of fossil fuel.

Retail prices in Germany for home storage systems with LIBs have decreased by about 50 % between 2013 and 2018 [45]. LIB prices are expected to fall significantly due to high demand in emerging applications and economies of scale [49], [51]. This price reduction forecast suggests that WPS based on PV systems and LIBs will become an economic solution for meeting water demand for internally displaced people and refugee camps, communities living in off-grid areas (especially in developing countries), as well as for agriculture. The use of batteries in PVWPS ensures the availability of water even at night and during periods of low light and cloudy weather [12]. Additional benefits can be achieved if excess energy stored in the LIB is used for other purposes: such as small appliance battery charging, lighting, and cooling. The challenge of combining new energy technologies opens new opportunities for long-term sustainability for humanitarian initiatives while improving the living conditions of the communities mentioned above.

IV. DESIGN AND CHARACTERIZATION OF A PV WATER PUMPING FACILITY WITH LITHIUM-ION BATTERY

In the PVWPS + LIB mode, the ac input of the VSD is connected to the back-up ac output of a hybrid inverter (the PCU) as shown in FIGURE 9. The control of the hybrid inverter decides the flow of energy between the PV modules, LIB, and the VSD. Several devices are included in the facility to protect and isolate the different parts of the system: FS1 is a fused disconnect switch mounted between the PV field and the hybrid inverter; and ACB* are the automatic circuit breakers mounted at the connections of the hybrid inverter with the battery (ACB1), the back-up output (ACB2), and the on-grid port (ACB3). The on/off switch mounted in the VSD is used to ensure a smooth pumping start/stop and so avoiding water hammers in the hydraulic circuit. If the PCU is configurated into the off-grid mode, the grid connection is not used and ACB3 can be opened. ACB3 was always open during the PVWPS + LIB tests. Magnitudes acquired in the battery-based solution and used to analyze the behavior of the system are detailed in FIGURE 10, where the hybrid inverter is denoted as the power converter unit (PCU) added in the facility to support the inclusion of the LIB in the PVWPS scheme. The output of the PCU coincides with the input of the VSD.

To analyze the PVWPS + LIB operation, two consecutive days with different weather conditions (09/24 and 09/25) were selected. The values of the more relevant parameters estimated during these two days, together with the average values for a set of 15 days, are detailed in Table 4. The *GI* profile on 09/24 corresponds to a cloudy day, while 09/25 is a sunny day. These two days were selected because they present irradiance characteristics reasonably similar to the days used for the direct pumping mode analysis. This can be verified by comparing the PSH values, being 2.01 and 6.54 on 10/02 and 10/03 respectively (DPVWPS), and 2.18 and 6.42 on 9/24 and 9/25 respectively (PVWPS + LIB). Likewise, the other corresponding values presented in Table 2 and Table 4 can be compared due to the similarities of the selected days.

Some of the benefits of the PVWPS + LIB facilities can be verified by analyzing the plots in FIGURE 11 in which *GI*, P_{PV}, SOC, and *Q* Values during 09/24 and 09/25 are represented in the graphic user interface built in Grafana [42]. FIGURE 11-d shows how the flow rate remains constant during all the pumping intervals, with the VSD operating at its rated conditions, and where electro-mechanical efficiency is at its maximum values.

The comparison of *GI* (FIGURE 11-a) and P_{PV} (FIGURE 11-b) shows the MPP tracking of the PV field for all levels of irradiance and without the irradiance threshold common in the DPVWPS facilities. All the energy produced by the PV field can be stored in the battery or used for

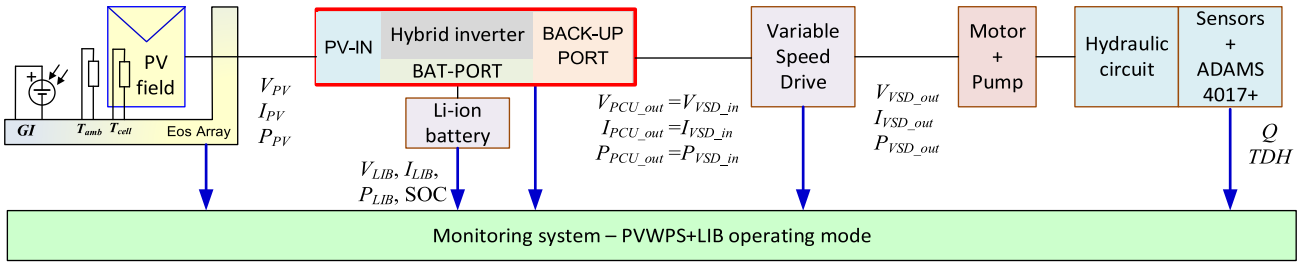

FIGURE 10. Main magnitudes measured by the monitoring system in the PVWPS + LIB facility.

TABLE 4. Values obtained for the battery-based solution on September 24 and 25 and average values considering 15 days.

	9/24	9/25	$AV_{15\ days}$
PSH	2.18	6.42	5.26
TDH_{AV} (m)	23.51	23.56	23.57
V_d (m^3/d)	8.49	48.90	33.39
E_{PV} (kWh/d)	3.47	13.47	9.50
PR_{PV} (%)	65.21	86.02	72.73
ΔE_{LIB} (kWh/d)	-0.21	-0.32	-0.17
E_{LIB_cha} (kWh/d)	1.76	3.04	2.83
E_{LIB_dis} (kWh/d)	-1.97	-3.36	-3.00
SOC_{ini} (%)	33.00	41.00	54.48
SOC_{end} (%)	41.00	42.00	54.45
E_{PCU_in} (kWh/d)	3.59	13.77	9.62
E_{VSD_out} (kWh/d)	1.63	9.40	6.45
$PR_{PCU+VSD}$ (%)	45.25	68.29	64.71
E_h (kWh/d)	0.55	3.14	2.15
PR_{mp} (%)	33.67	33.41	33.44
$PR_{PVWPS+LIB}$ (%)	15.77	23.32	21.71
$PR_{syst\ (LIB)}$ (%)	1.62	3.15	2.52
$\eta_{PCU+VSD\_max}$ (%)	80.19	76.15	78.50
$\eta_{PCU+VSD\_AV}$ (%)	75.17	74.13	74.27
η_{mp_max} (%)	33.91	35.24	35.17
η_{mp_AV} (%)	33.47	33.40	33.25
$\eta_{PVWPS+LIB\_max}$ (%)	25.34	25.29	26.75
$\eta_{PVWPS+LIB\_AV}$ (%)	25.15	24.80	24.86
Pumping time	56 min	311 min (5h:11min)	215 min (3h:35min)

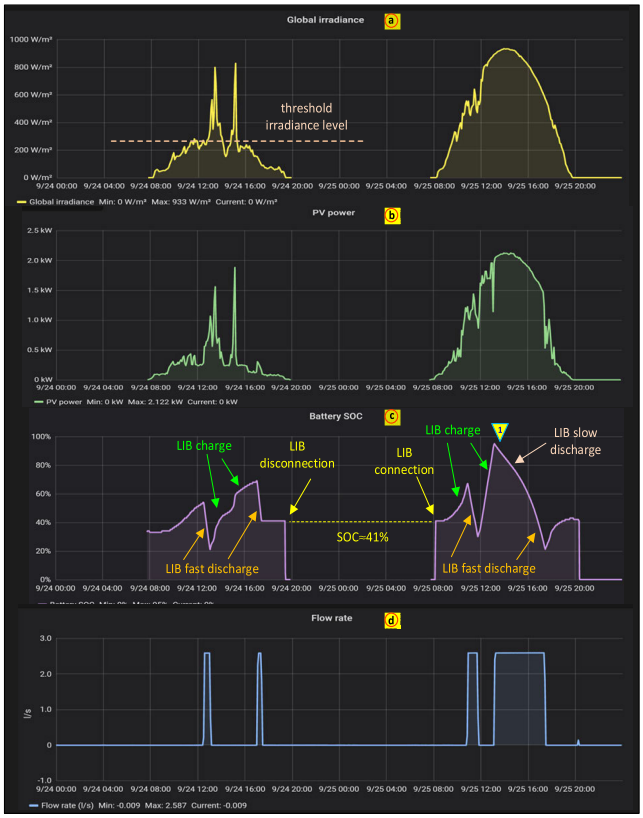

FIGURE 11. Values obtained with the battery-based solution (from 09/24 00:00 to 09/25 23:59).

pumping water by activating the VSD and so optimizing the use of the PV modules.

In the PVWPS + LIB operation mode, the LIB is charged with the energy not used and this is discharged when *GI* cannot provide enough P_{PV} to meet pump demand. The pump operates at its rated values and the energy in the LIB prevents pump stop/start cycles caused by the passage of clouds. Although *GI* shows significant variations during the day 9/24 and only exceeds GI_{thre_start} during two short time intervals, it can be seen that Q is equal to 2.61 L/s during the pumping intervals shown in FIGURE 11 and the total pumped volume is 8.36 m^3. The activation of the WPS ($Q >$ 0 L/s) coincides with a decrease in the SOC as the power coming from the LIB is necessary to maintain motor-pump power consumption. The pumping intervals during the various experiments carried out on the PVWPS + LIB facility were generally selected according to the following main criteria:

- The SOC must never reach 100% to avoid the loss of PV energy that cannot be stored, and this can be easily achieved thanks to the coupling between the PV array and the VSD.
- The minimum SOC recommended by the LIB manufacturers is set at about 20 %, and so the WPS must be disconnected before this trigger level to avoid damaging the LIB.
- Pumping periods should be chosen to coincide with high levels of *GI*. In this way, the energy flow towards the battery is reduced and therefore losses decrease. The battery can be charged at the beginning and end of the day,

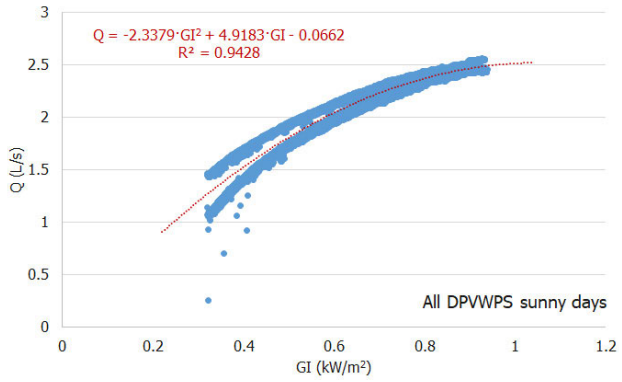

FIGURE 12. Estimation of flow from irradiance in the direct solution.

when P_{PV} is lower. An example is shown in the pumping interval from 13:10 to 15:30 on 9/25 – when the PV power is greater than 2 kW and the battery discharge shows a small discharging slope when compared with other discharging intervals also shown in FIGURE 11.

During the days when the tests were carried out with the PVWPS + LIB mode, an attempt was made to maintain the same SOC at the beginning and end of the day (which enables establishing daily energy balances in the system) (FIGURE 11-c).

A fitting model was used to predict the hypothetical Q values that could be obtained with the direct solution (FIGURE 12). Cloudy days were eliminated from the adjustment and in this way the "noise" in GI caused by the heterogeneity of the passage of clouds was discarded. With this model, the values of V_d pumped with the direct solution can be estimated, obtaining a V_d of 8.28 m^3 for day 9/24. Although the GI profile on 9/24 corresponds to a cloudy day, this result could be considered an adequate estimate as it was calculated without considering the delay in pump start-up that the VSD control could introduce to avoid start/stop cycles on cloudy days (as shown at the beginning of 10/2 in FIGURE 4). For the PVWPS + LIB mode, the value obtained of $V_{d9/24} =$ 8.36 m^3, was slightly higher than that estimated for the direct solution with comparable GI levels. This could suggest that the use of a battery improves the pumped volume under cloudy conditions.

FIGURE 13 shows the power of the various components of the battery-based solution and the corresponding efficiencies for a one-minute recording interval on 9/25 in which the system is pumping at rated conditions ($f_{VSD} = 50$ Hz). The changes in powers, efficiencies, SOC, and GI values on 9/25 from 08:00 to 20:00 are shown in FIGURE 14, where the powers remaining constant during the pumping intervals ($Q \approx 2.61$ L/s) are represented with dashed lines. All the represented conversion efficiencies remain practically constant throughout each pumping interval and are independent of GI. The upper part of this figure shows how the LIB output power ($P_{LIB} < 0$) varies to compensate P_{PV} to maintain P_{PCU_in} constant, and so that P_{VSD} and P_h are also constant when the system is pumping. To maintain the pumping system at its rated conditions, the battery provides power from the moment the pumping starts and this causes the SOC to decrease (the decrease being faster the lower the radiation levels). The efficiencies in the conversion in the PCU + VSD blocks, motor-pump, and PVWPS + LIB group are respectively 74.7 %, 33.3 %, and 24.9 % when the WPS is in operation (FIGURE 13) This corresponds to those values shown in FIGURE 14 at 16:00h and remain practically constant throughout the pumping period. Nevertheless, the efficiency in the PV conversion, or in the charging/discharging processes in the LIB, vary continuously with GI throughout the day. The difference between P_{PV} and the power in the LIB (P_{LIB}) when $P_h = 0$ W corresponds to the power losses in the dc/dc converter that manages the LIB charging.

Two power sources are connected to the PCU inputs: the PV generator and the LIB. The power of the LIB (P_{LIB}) is considered positive during the charging process from the PV generator. The power in the PCU input (P_{PCU_in}) is used to generate the ac single-phase waveform that feeds the VSD (AC2 BACK-UP block in FIGURE 9) and is calculated for each recording interval as follows:

$$P_{PCU_{in},k} = P_{PV,k} - P_{LIB,k} \tag{5}$$

From a preliminary study being conducted on the efficiency of LIB (η_{LIB}), an average efficiency of 81.1 % was obtained during a full charging process (SOC from 0 % to 100 %) using the power delivered by the PV generator with values of $\eta_{LIB,k}$ varying between 68.3 % and 97.2 %.

Two intervals of pumping were established during 9/25, from 10:54 to 11:47 (53 min) and from 13:10 to 17:28 (258 min). When the WPS is disconnected ($Q = 0$ L/s) the energy generated by the PV field is used to recharge the LIB ($P_{LIB} > 0$ W during charging) and P_{VSD_out} and P_h are null. Several problems are identified after the analysis of the signals included in FIGURE 14, related with:

- Operation of the MPPT algorithm during the charging intervals of the LIB.
- Values provided by the hybrid inverter for P_{PCU_in} and P_{PCU_out}.
- Stand-by consumption of the VSD and the hybrid inverter.

Although the PCU that manages the PV generation includes an MPPT algorithm, the average values of PR_{PV} in the direct solution (Table 2) are greater than those obtained with the battery-based solution (Table 4). Specifically, in the facility under study, the average values of PR_{PV} are 88.10 % and 72.73 % in DPVWPS and PVWPS + LIB, respectively. Differences are greater on sunny days (the sunnier the day, the greater the differences). Nevertheless, on cloudy days the battery-based solution takes advantage of a battery with higher PR_{PV} (65.21 % with battery storage versus a 41.21 % with operation in direct mode on selected days). These differences are caused by the improper operation of the MPPT algorithm in the battery-based solution when P_{PV} is used

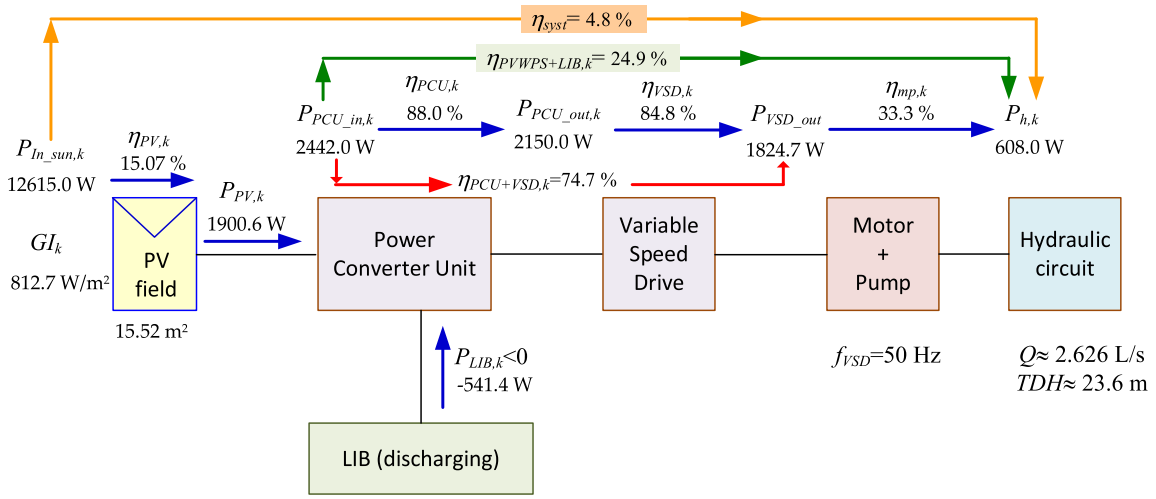

FIGURE 13. Power and efficiency values in the battery-based solution at 16:00 on 9/25.

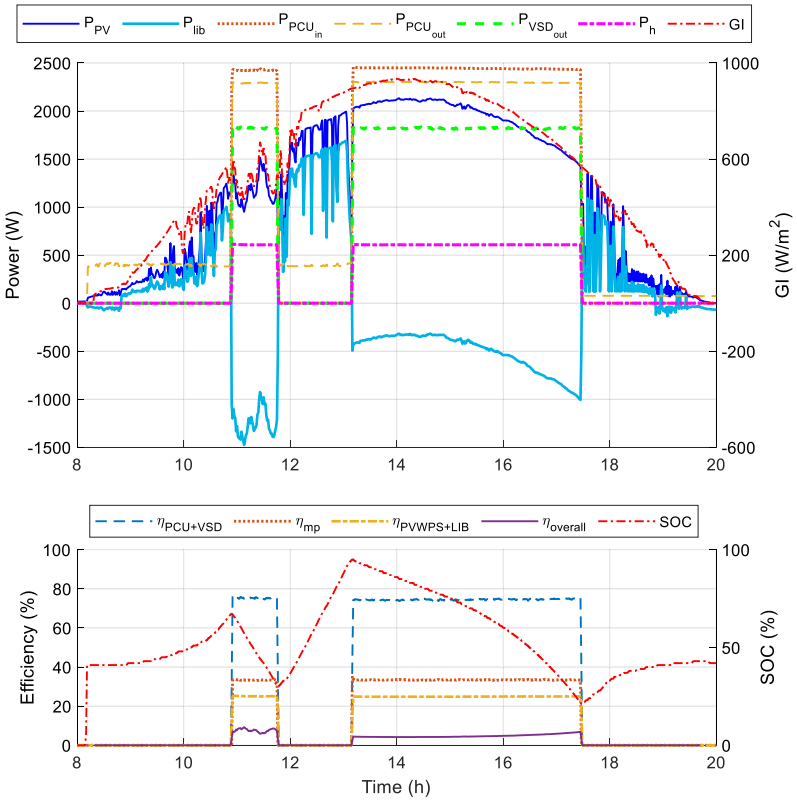

FIGURE 14. Powers (PV, battery, input and output of the power converter unit, VSD output, and hydraulic), efficiencies (power converter unit and VSD, motor-pump, $\eta_{PVWPS+LIB}$, $\eta_{overall}$), state of charge in the battery, and irradiance values obtained with the battery-based solution on 9/25 from 08:00 to 20:00.

to recharge the LIB, as can be seen in FIGURE 14, when $P_h = 0$ W, and in FIGURE 15 where powers and GI values are represented in the time interval from 17:30 to 20:00. Significant P_{PV} variations in parallel with smooth GI fluctuations can be observed in both FIGURE 14 and FIGURE 15. While in these two figures the recording interval was one minute, Grafana adjusts the recording interval depending on the time interval that is presented and the available size of the application window on the screen. This procedure results in recording intervals in the range of five minutes or more and an averaging of the signals. With longer recording intervals, as is common in commercial monitoring systems, the curves present a smoother variation that does not reveal any anomaly or irregularity in the magnitudes, and so only a low performance ratio in the installation will indicate that something can be improved in the facility.

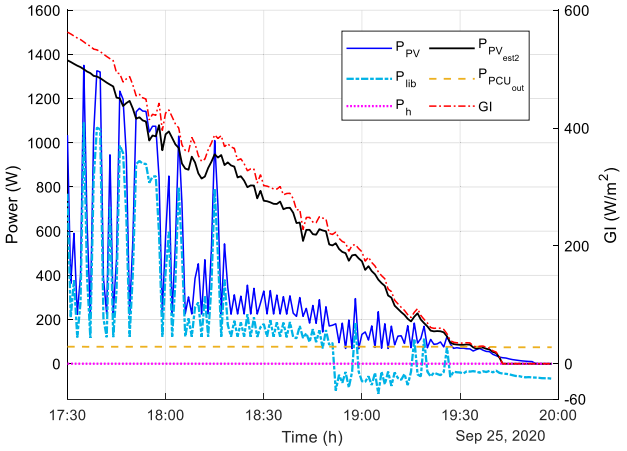

FIGURE 15. Powers (PV, PV estimation 2, battery, PCU output, and hydraulic) and irradiance values obtained with the battery-based solution on 9/25 from 17:30 to 20:00.

TABLE 5. Relationship between PV power and irradiance during the time interval from 17:35 to 17:46 (part of the first interval after pumping stops) on 9/25.

Time	P_{PV} (W)	GI (W/m^2)	P_{PV} / GI	SOC (%)
17:35:00	1330.71	546.25	2.44	23.0
17:36:00	519.06	541.97	0.96	24.0
17:37:00	212.90	539.06	0.39	24.0
17:38:00	1032.74	533.97	1.93	24.0
17:39:00	1298.42	532.77	2.44	24.8
17:40:00	1297.00	529.78	2.45	25.3
17:41:00	292.39	525.61	0.56	26.0
17:42:00	212.65	521.42	0.41	26.0
17:43:00	893.35	517.77	1.73	26.0
17:44:00	211.26	514.32	0.41	26.0
17:45:00	459.94	493.61	0.93	26.6
17:46:00	1208.23	492.23	2.45	27.0

Three intervals can be distinguished in FIGURE 15:

- From 17:30 to 18:24, P_{PV} varies between the expected value according to GI, in accordance with the fitting analysis performed previously, and a base value located around 200 W, as can be seen in Table 5.
- From 18:24 to around 19:15 P_{PV} values vary between 200 W and 300 W and the proportionality diminishes with the GI values.
- After 19:15 GI values are below 100 W/m^2 and P_{PV} again becomes proportional to GI with values near to those obtained with the estimations calculated from the fitting function.

The oscillations shown by P_{PV} when the WPS is not pumping suggest a low performance in the use of the available solar energy. Therefore, an assessment of the energy lost between 17:30 and 19:25 on 9/25 is performed using the linear fitting described in Section II. The estimated potentially available P_{PV} values when $k_{GI2} = 2.40$ is used are included in FIGURE 15 (P_{PV_est2}).

When analyzing the time interval from 17:28 to 19:25 on 9/25, the PV energy obtained from estimations using $k_{GI1} = k_{GI\_all}$ and k_{GI2} are equal to 1368 Wh and 1519 Wh respectively, while the real PV generated energy is 758 Wh. The loss

TABLE 6. Estimation of the PV energy generated using $k_{GI\_all} = 2.2747$ on September 24 and 25, and average value considering 15 days for the battery-based solution.

	9/24	9/25	$AV_{15\ days}$
E_{PV} (kWh/d)	3.47	13.47	9.50
E_{PV_est1} (kWh/d)	4.96	14.60	11.44
ΔE_{PV_est1} (%)	142.9	108.3	128.7

of energy due to the incorrect operation of the MPP tracking can reach 761 Wh for k_{GI2}, which represents twice the energy actually generated in this interval and constitutes an increase of 5.78 % when compared with the total PV energy produced ($E_{PV9/25} = 13.47$ kWh, as indicated in Table 6). Considering that $PR_{PVWPS+LIB} = 23.32$ % on 9/25 (Table 4), the surplus hydraulic energy in this interval is 177.4 Wh. The value of P_h during the pumping intervals on 9/25 is 603 W with $Q_{AV} = 2.61$ L/s. A surplus pumping time of 17.65 minutes can then be obtained, which represents a surplus pumped volume of 2.76 m^3. Table 6 shows that the average ΔE_{PV_est1} with a correct operation of the MPPT is estimated at 128.7 %.

The other issues identified in FIGURE 14 are related to the measurement technique used by the hybrid inverter and the VSD stand-by consumption. As can be verified, the values of P_{PCU_in} and P_{PCU_out} provided by the hybrid inverter to the monitoring system are not correctly measured. During the first two intervals without pumping (from 8:00 to 10:54 and from 11:47 to 13:10) the values of P_{PCU_out} (green dashed line) are greater than the values of P_{PCU_in} (red dashed line) and are around 400 W and 110 W respectively. A Fluke 435-SII power quality analyzer was used to verify the power measurements, and revealed that the value measured in the output terminals of the PCU corresponding to the stand-by consumption of the VSD, represented an active power of 40 W and an apparent power of 300 VA. Because this consumption of the VSD represents a loss of energy when the WPS is not pumping, the breaker ACB2 in FIGURE 9 was disconnected after 17:30, and this decreased the value of P_{PCU_out} to around 70 W, as is shown in FIGURE 15. This value corresponds to the stand-by consumption of the hybrid inverter. The measurement error was also corrected in the value of $P_{PCU\_out} = 2150$ W presented in FIGURE 13 and which according to the measurement of the hybrid inverter was 2289 W. The problems regarding the stand-by consumption of the hybrid inverter, mainly observed during the night, were reported in [42]. The decrease in the battery SOC during nights (around 25 %) is avoided by disconnecting the hybrid inverter when the WPS is not in operation.

Although an increase in E_{PV} values of between 4 % and 6 % was expected with better management of incoming solar energy in the battery-based solution, the problems found in the MPPT algorithm resulted in a decrease in PR_{PV} values that penalizes the overall system. The combination of low PR_{PV} with the lower $\eta_{PVWPS+LIB}$ results in a reduction of pumped volume on average and sunny days, and a benefit is only produced on cloudy days or days with frequently alternating sunny and cloudy periods.

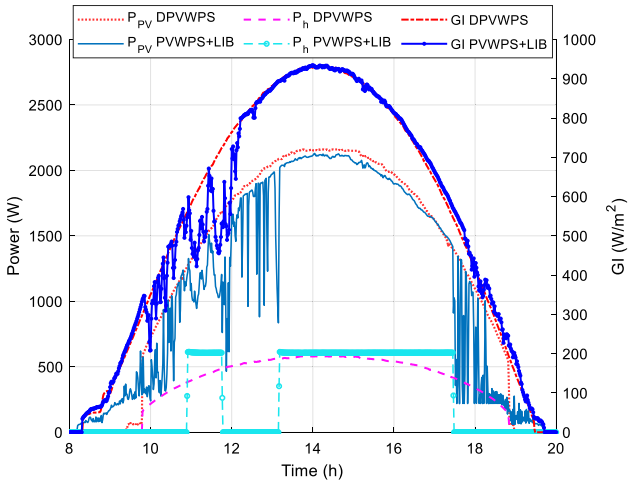

FIGURE 16. PV power, hydraulic power and irradiance values on 9/25 (battery-based solution) and on 10/3 (direct solution).

V. DISCUSSION OF THE EXPERIMENTAL RESULTS: DPVWPS VS PVWPS + LIB

Magnitudes shown in FIGURE 16 enable a comparison of the behavior of the direct and the battery-based schemes for two similar sunny days (10/3 and 9/25) with 6.54 and 6.42 PSH respectively. The MPPT operation in the battery-based solution during the pumping intervals is quite similar to that shown for the direct solution, and the same should also occur when pumping stops. Without considering the MPPT inconvenience concerning the hybrid inverter, the main difference between both modes of operation lies in the P_h plot, where the typical bell shape in the direct solution turns into a rectangular shape because the WPS is operating at rated conditions. The small difference between the P_{PV} values in the central hours of the days must be attributed to the different T_{cell} for each day. Around noon for $GI \approx 932$ W/m^2, the P_{PV} and T_{cell} values acquired are 2160 W and 39.4 °C for the direct solution, and 2073 W and 47.3 °C for the battery-based solution. The difference of 87 W is explained by the 7.9 °C of difference in T_{cell} if the value of $\gamma_{P_{MPP}}$ in Table 1 is considered.

The average value of $PR_{PVWPS+LIB}$ is 21.71 % (Table 4), a lower value than the 27.95 % obtained for PR_{DPVWPS} (Table 2). This decrease can be explained by the losses produced by the additional components in the battery-based solution: the hybrid inverter (or the PCU) and the LIB. When average efficiencies are considered, the difference is less than 3 % (being $\eta_{DPVWPS\_AV} = 27.82$ % and $\eta_{PVWPS+LIB\_AV} = 24.86$ %).

An approach to compensate for the reduction of $PR_{PVWPS+LIB}$ is to increase the installed PV power. Oversizing the PV field will produce extra energy that compensates for the greater losses of the battery-based solution. The PV field oversizing factor (OF) can be calculated in an initial approach as the ratio between PRs as follows:

$$OF = \frac{PR_{DPVWPS}}{PR_{PVWPS+LIB}} \tag{6}$$

With the values shown in Table 2 and Table 4, OF is equal to 1.28, and so a PV field with 3.12 kW$_{pk}$ (eight modules of 390 W$_{pk}$ in series) will be needed for the battery-based solution to pump the same V_d. Knowing that $A_{PV} = 15.52$ m^2 and $GI_{STC} = 1000$ W/m^2, the PV module efficiency (η_{PV}) must be greater than 20.12 %. Many manufacturers are now offering PV modules with 72 cells in series with maximum values of η_{PV} greater than 21 % (with a cost of about 0.22 €/W$_{pk}$). Therefore, at an extra cost of around €150, a 3.12 kW$_{pk}$ battery-based solution can compensate for extra losses in the system and pump the same daily volume as a 2.44 kW$_{pk}$ direct solution – but with the advantages of a system with batteries.

The effect of the improper operation of the MPPT algorithm is included in the PR_{syst} (%) value as it changes from 3.87 % in the direct solution to 2.52 % in battery-based solution (a reduction of 35 %). One effect of the lower utilization of solar energy is observed in pumped volume. The average pumped volume in the direct solution is 55.34 m^3/day compared with the 33.39 m^3/day in the battery-based solution and this represents a decrease of 40 % (considering in both cases an average day with 5.26 PSH). Nevertheless, the pumped volume with the battery-based solution can scarcely reach that obtained with the direct solution for the following reasons:

- The study is performed using the same PV field, so both systems would manage the same amount of E_{PV} (assuming a correct operation of the MPPT).
- The value of $PR_{PVWPS+LIB}$ is 22.4 % lower than PR_{DPVWPS}.
- The threshold irradiance levels of the direct solution are quite low ($GI_{thre\_start} \approx 300$ W/m^2 and $GI_{thre\_stop} \approx 200$ W/m^2). This means that the energy stored in the LIB when $GI < GI_{thre\_**}$ is insufficient to compensate for the reduction of $PR_{PVWPS+LIB}$ due to losses in the additional devices in the system (hybrid converter and LIB).

The values of GI_{thre_*} in a DPVWPS mainly depend on the selected pump and the TDH. The conditions configured in the facility during the tests correspond to the minimum possible TDH that yields a minimum value of GI_{thre_*}. GI_{thre_*} depends on the minimum power required to pump at a given head and increases with the pump head. The minimum power practically triples from pumping at a head of 24 m (0.26 kW) to a head of 54 m (0.73 kW) for the pump of 0.75 kW used in [52]. A greater value of TDH will increase GI_{thre_*} which will increase the amount of energy stored in the LIB while GI $< GI_{thre\_*}$. In this way, pumping operating conditions could be reached in which the daily volume in the battery-based solution exceeds that obtained with the direct solution.

By taking advantage of the extended characteristics in the PV input of the hybrid inverter Table 7 with respect to those of the VSD (Table 1), a greater PV oversizing factor can be used, although the system would require a higher capacity battery to store the surplus energy that could be produced. Reviewing the values included in Table 7 shows that two

TABLE 7. Electrical characteristics of the PV input of the hybrid inverter.

P_{MPP_hyb}	V_{OC_hyb}	V_{MPP_hyb}
4600 W_{pk}	580 V	170~500 V
I_{SC_hyb}	I_{MPP_hyb}	
13.8/13.8 A	11/11 A	

strings with 8 PV modules in series could be connected to the hybrid inverter, thereby doubling the peak power of the PV field and so doubling the PV energy generated.

Considering the E_{PV} values in Table 2 and Table 4, it is considered that an LIB with 15 kWh could store the energy produced by the extra string most of the year. Considering that $PR_{PVWPS+LIB\_AV} = 21.71$ %, the 15 kWh stored in the LIB can be converted to $E_h \approx 3.25$ kWh. Using the values shown in FIGURE 13 ($P_h = 603$ W and $Q = 2.61$ L/s) the extra pumping time due to the additional string is 5.4 hours, which represents an increase in pumped volume of 50.74 m^3. Economic issues, combined with water demands, must be used to define the final characteristics of the battery-based facility. An oversizing of the PV field and the LIB could be considered if a surplus of stored energy is needed for uses other than the WPS (such as small appliance battery charging and lighting). In these cases, it will be necessary to add some kind of energy manager to decide the amount of energy that can be used for these other purposes.

PVWPS + LIB systems are easily scalable and so the system can be configured to provide considerable autonomy under low irradiation conditions. With the objective of reducing the size of the photovoltaic field and the battery, it is common in off-grid applications to find an auxiliary generator that can be connected when irradiance does not enable the operation of the DPVWPS facility. The VSD used in the direct solution includes a single-phase ac input that is compatible with the voltage provided by an auxiliary generator. In the battery-based solution, the single-phase output of the auxiliary generator can be connected to the grid input of the hybrid inverter to provide energy to the VSD and the LIB. Charging current can be configured to avoid overloading the auxiliary generator. An energy manager would be needed in this case to control the activation of the auxiliary generator, set the maximum LIB charging current, and so on.

VI. CONCLUSION

The main drawbacks of the battery-based solution when compared with the direct solution are related to the energy losses associated with the hybrid inverter and LIB charging and discharging processes. While the average value of PR_{DPVWPS} is around 28 %, the average $PR_{PVWPS+LIB}$ reaches values close to 22 % with the WPS operating at rated conditions. The PV field used in the comparison of the direct and battery-based solution is the same and was designed considering the constraints imposed by the VSD. This means that for the same energy input the battery-based solution will produce less volume due to the reduction of $PR_{PVWPS+LIB}$ when compared to PR_{DPVWPS}.

This reduction in the performance ratio can easily be compensated if the PV field power is increased. A 30 % oversizing of the PV field in the battery-based solution can compensate for the extra losses of this system and pump the same daily V_d as the direct solution. Greater oversizing factors can be used when the extended characteristics of hybrid inverters are used for the design of the PV field and the LIB and this will enable pumping time to be extended.

The inclusion of a battery prevents the pump stopping due to passing clouds and this reduces damage in the motor-pump group and cuts O&M costs. A battery also enables the WPS to be operated at any time, although efficiency improves if the pumping intervals coincide with sunny hours and there is little energy flow in the battery. Some common problems related to the direct solution, such as clipping at noon or threshold irradiance level at sunrise and sunset, are avoided with a battery-based solution. All the energy losses related to these topics can be stored in the LIB and used for pumping.

Several problems were found in the PVWPS + LIB facility used in the experimental parts of the study. The main problem found is related to an improper operation of the algorithm included in the hybrid inverter that implements the tracking of the PV field MPP. Increases in daily pumped volume in the range of 8 % to 20 % can be expected with proper MPPT operation. Other problems are related to energy consumption in the stand-by mode of the hybrid inverter and VSD. The stand-by mode of the VSD demands power to the back-up output of the hybrid inverter throughout the day. This consumption can be avoided if the VSD is disconnected from the back-up output when the WPS is not pumping. Stand-by consumption by the hybrid inverter is also avoided by completely disconnecting the hybrid inverter during the night when the WPS is not going to be in operation.

The approach for the conversion of a direct solution to a corresponding battery-based scheme presented in this work is valid for commercial DPVWPS solutions proposed by other manufacturers (such as Grundfos and ABB). Given the results obtained and the technological evolution in the field of hybrid inverters and LIBs since this project started in 2018, future actions are being evaluated to improve the results obtained with the PVWPS + LIB facility. These actions include: analyzing the operation of the WPS to improve the efficiency in the battery-based solution; using a hybrid inverter with a proper operation of the MPPT for the conditions imposed in the battery-based solution to assemble a hybrid inverter that supports the use of high-voltage LIBs; and using a lower rated pump in the battery-based solution that can work for longer periods to extract the same daily volume as the direct solution.

APPENDIXES

Supplementary data to this article can be found online in the IEEE Xplore in the MEDIA section.

NOMENCLATURE

ac	Alternate current
ADC	Analog-to-digital converter
AM	Air mass
AV	Average (subscript)
BMS	Battery management system
c−Si	Crystalline Silicon
cha	Charge of the battery (subscript)
dc	Direct current
DG	Distributed generation
DGT	Digit
dis	Discharge of the battery (subscript)
DPVWPS	Direct photovoltaic water pumping system
E_{**}	Energy in **
EL	Energy losses
ESS	Energy storage systems
est	Estimated (subscript)
f_{VSD}	Frequency of the three-phase voltages in the VSD output
g	Acceleration of gravity
GI	Global irradiance (in W/m^2)
GUI	Graphic user interface
h	Hydraulic (subscript)
H_i	Daily solar energy received by the photovoltaic modules or irradiation
HEL	Hydraulic equivalent load (in m^4/day)
hyb	Hybrid (subscript related to the hybrid inverter)
I_{**}	Current in device *∗ or current in conditions *∗
I_{SC}	Short-circuit current
LIB	Lithium-ion battery
max	Maximum (subscript)
min	Minimum (subscript)
min	Minute
MPP	Maximum power point
MPPT	Maximum power point tracking
mp	Motor-pump (subscript)
NOCT	Normal operating cell temperature
OV	Overvoltage
P_{**}	Power in device ** or power in conditions **
PC	Personal computer
PCU	Power converter unit (use for the combination of hybrid inverter plus VSD)
PF	Power factor
PF_m	Power factor of the motor installed in the motor-pump group
pk	Peak (subscript)
PL_{**}	Power losses in **
PR_{**}	Performance ratio in device ** (quotient of energies)
PSH	Peak sun hours (1 PSH = 1 kWh/m^2)
PV	Photovoltaic
PVWPS	Photovoltaic water pumping system
PVWPS + LIB	Photovoltaic water pumping system with storage in a lithium-ion battery
Q	Flow rate
RDG	Reading
RE	Renewable energies
rpm	Revolution per minute
R_{Tem}	Terminal resistance for the RS485 bus
SOC	State of charge
SOH	State of health
STC	Standard test conditions (1.5 AM, T_{cell} = 25 °C, and 1000 W/m^2)
T_{amb}	Ambient temperature (°C)
T_{cell}	PV cell temperature (°C)
TDH	Total dynamic head
thre	Threshold (subscript)
t_k	Recording interval
T_w	Water temperature
V_d	Total volume of water pumped in a day
V_{**}	Voltage in device ** or voltage in conditions **
V_{OC}	Open circuit voltage
VSD	Variable speed drive
WPS	Water pumping system
α	Current temperature coefficient of the PV module (in %/K)
$\beta_{V_{MPP}}$	MPP voltage temperature coefficient of the PV module (in %/K)
$\beta_{V_{OC}}$	Open circuit voltage temperature coefficient of the PV module (in %/K)
γ	Power temperature coefficient of the PV module (in %/K)
η_{**}	Efficiency in device ** (quotient of powers)

ACKNOWLEDGMENT

To the Vice-Chancellor of Infrastructure at the UPV for the financial support that enabled the electrical installation of the project to be completed.

To the Goodwe company for the donation of a hybrid inverter, even though the company was aware that the inverter would be used in extreme conditions for which it was not designed. The project could not have started without its contribution, and we would not have acquired the knowledge that will enable them to progress in these humanitarian applications.

To the Carlos Gavazzi company (monitoring and data acquisition system) for its involvement in the project.

To Alberto Ibáñez Llario, Global Solar Energy & Water Advisor at the United Nations Agency for Migration for introducing them to the field of humanitarian aid.

REFERENCES

[1] M. Aliyu, G. Hassan, S. A. Said, M. U. Siddiqui, A. T. Alawami, and I. M. Elamin, "A review of solar-powered water pumping systems," *Renew. Sustain. Energy Rev.*, vol. 87, pp. 61–76, May 2018, doi: 10.1016/j.rser.2018.02.010.

[2] P. K. S. Rathore, S. S. Das, and D. S. Chauhan, "Perspectives of solar photovoltaic water pumping for irrigation in India," *Energy Strategy Rev.*, vol. 22, pp. 385–395, Nov. 2018, doi: 10.1016/j.esr.2018.10.009.
[3] J. Meyer and S. von Solms, "Solar powered water security: An enabler for rural development in Limpopo South Africa," *IEEE Access*, vol. 6, pp. 20694–20703, Apr. 2018, doi: 10.1109/ACCESS.2018.2805367.
[4] A. W. Kiprono and A. I. Llario, *Solar Pumping for Water Supply: Harnessing Solar Power in Humanitarian and Development*, 1st ed. Rugby, U.K.: Practical Action Publishing, 2020.
[5] T. Khatib and D. H. Muhsen, "Chapter 1—Introduction," in *Photovoltaic Water Pumping Systems*, 1st ed., T. Khatib and D. H. Muhsen, Eds. New York, NY, USA: Academic, 2021, pp. 1–4.
[6] M. Tvaronavičienė, J. Baublys, J. Raudeliūnienė, and D. Jatautaitė, "Chapter 1—Global energy consumption peculiarities and energy sources: Role of renewables," in *Energy Transformation Towards Sustainability*, 1st ed., M. Tvaronavičienė, and B. Ślusarczyk, Eds. Amsterdam, The Netherlands: Elsevier, 2020, pp. 1–49.
[7] J. S. Ramos and H. M. Ramos, "Solar powered pumps to supply water for rural or isolated zones: A case study," *Energy Sustain. Develop.*, vol. 13, no. 3, pp. 151–158, Sep. 2009, doi: 10.1016/j.esd.2009.06.006.
[8] A. Allouhi, M. S. Buker, H. El-Houari, A. Boharb, M. B. Amine, T. Kousksou, and A. Jamil, "PV water pumping systems for domestic uses in remote areas: Sizing process, simulation and economic evaluation," *Renew. Energy*, vol. 132, pp. 798–812, Mar. 2019, doi: 10.1016/j.renene.2018.08.019.
[9] N. T. Argaw, *Renewable Energy Water Pumping Systems Handbook; Period of Performance: April 1–September 1, 2001*. CO, USA. [Online]. Available: https://www.osti.gov/servlets/purl/15008778 and https://www.osti.gov/biblio/15008778-renewable-energy-water-pumping-systems-handbook-period-performance-april-september, doi: 10.2172/15008778.
[10] S. S. Chandel, M. N. Naik, and R. Chandel, "Review of solar photovoltaic water pumping system technology for irrigation and community drinking water supplies," *Renew. Sustain. Energy Rev.*, vol. 49, pp. 1084–1099, Sep. 2015, doi: 10.1016/j.rser.2015.04.083.
[11] D. H. Muhsen, T. Khatib, and F. Nagi, "A review of photovoltaic water pumping system designing methods, control strategies and field performance," *Renew. Sustain. Energy Rev.*, vol. 68, pp. 70–86, Feb. 2017, doi: 10.1016/j.rser.2016.09.129.
[12] V. C. Sontake and V. R. Kalamkar, "Solar photovoltaic water pumping system—A comprehensive review," *Renew. Sustain. Energy Rev.*, vol. 59, pp. 1038–1067, Jun. 2016, doi: 10.1016/j.rser.2016.01.021.
[13] S. S. Chandel, M. N. Naik, and R. Chandel, "Review of performance studies of direct coupled photovoltaic water pumping systems and case study," *Renew. Sustain. Energy Rev.*, vol. 76, pp. 163–175, Sep. 2017, doi: 10.1016/j.rser.2017.03.019.
[14] M. Hadwan and A. Alkholidi, "Assessment of factors influencing the sustainable performance of photovoltaic water pumping systems," *Renew. Sustain. Energy Rev.*, vol. 92, pp. 307–318, Sep. 2018, doi: 10.1016/j.rser.2018.04.092.
[15] A. Mokeddem, A. Midoun, D. Kadri, S. Hiadsi, and I. A. Raja, "Performance of a directly-coupled PV water pumping system," *Energy Convers. Manage.*, vol. 52, no. 10, pp. 3089–3095, Sep. 2011, doi: 10.1016/j.enconman.2011.04.024.
[16] B. G. Belgacem, "Performance of submersible PV water pumping systems in tunisia," *Energy Sustain. Develop.*, vol. 16, no. 4, pp. 415–420, Dec. 2012, doi: 10.1016/j.esd.2012.10.003.
[17] R. Dharavath, I. J. Raglend, S. P. Karthikeyan, and J. B. Edward, "A bibliographical survey on integration of hybrid renewable energy sources with diesel generator and storage system," *J. Eng. Sci. Technol. Rev.*, vol. 11, no. 5, pp. 61–75, Oct. 2018, doi: 10.25103/jestr.115.08.
[18] R. Siddaiah and R. P. Saini, "A review on planning, configurations, modeling and optimization techniques of hybrid renewable energy systems for off grid applications," *Renew. Sustain. Energy Rev.*, vol. 58, pp. 376–396, May 2016, doi: 10.1016/j.rser.2015.12.281.
[19] H. Rezk, M. Al-Dhaifallah, Y. B. Hassan, and H. A. Ziedan, "Optimization and energy management of hybrid photovoltaic-diesel-battery system to pump and desalinate water at isolated regions," *IEEE Access*, vol. 8, pp. 102512–102529, 2020, doi: 10.1109/ACCESS.2020.2998720.
[20] L. da Silva Lima, M. Quartier, A. Buchmayr, D. Sanjuan-Delmás, H. Laget, D. Corbisier, J. Mertens, and J. Dewulf, "Life cycle assessment of lithium-ion batteries and vanadium redox flow batteries-based renewable energy storage systems," *Sustain. Energy Technol. Assessments*, vol. 46, Aug. 2021, Art. no. 101286, doi: 10.1016/j.seta.2021.101286.
[21] S. Koohi-Fayegh and M. A. Rosen, "A review of energy storage types, applications and recent developments," *J. Energy Storage*, vol. 27, pp. 1–23, Feb. 2020, doi: 10.1016/j.est.2019.101047.
[22] A. Abdon, X. Zhang, D. Parra, M. K. Patel, C. Bauer, and J. Worlitschek, "Techno-economic and environmental assessment of stationary electricity storage technologies for different time scales," *Energy*, vol. 139, pp. 1173–1187, Nov. 2017, doi: 10.1016/j.energy.2017.07.097.
[23] D. Groppi, A. Pfeifer, D. A. Garcia, G. Krajačić, and N. Duić, "A review on energy storage and demand side management solutions in smart energy islands," *Renew. Sustain. Energy Rev.*, vol. 135, pp. 1–14, Jan. 2021, doi: 10.1016/j.rser.2020.110183.
[24] S. S. Raghuwanshi and R. Arya, "Reliability evaluation of stand-alone hybrid photovoltaic energy system for rural healthcare centre," *Sustain. Energy Technol. Assessments*, vol. 37, pp. 1–9, Feb. 2020, doi: 10.1016/j.seta.2019.100624.
[25] T. Castillo-Calzadilla, C. M. Andonegui, M. Gomez-Goiri, A. M. Macarulla, and C. E. Borges, "Systematic analysis and design of water networks with solar photovoltaic energy," *IEEE Trans. Eng. Manag.*, early access, Nov. 28, 2019, doi: 10.1109/TEM.2019.2940340.
[26] A. Hamidat and B. Benyoucef, "Systematic procedures for sizing photovoltaic pumping system, using water tank storage," *Energy Policy*, vol. 37, no. 4, pp. 1489–1501, Apr. 2009, doi: 10.1016/j.enpol.2008.12.014.
[27] M. Pardo, R. Cobacho, and L. Bañón, "Standalone photovoltaic direct pumping in urban water pressurized networks with energy storage in tanks or batteries," *Sustainability*, vol. 12, no. 2, pp. 1–20, Jan. 2020, doi: 10.3390/su12020738.
[28] A. Mohammedi, D. Rekioua, T. Rekioua, and N. E. Mebarki, "Comparative assessment for the feasibility of storage bank in small scale power photovoltaic pumping system for building application," *Energy Convers. Manage.*, vol. 172, pp. 579–587, Sep. 2018, doi: 10.1016/j.enconman.2018.07.056.
[29] I. Yahyaoui, A. Atieh, F. Tadeo, and G. M. Tina, "Energetic and economic sensitivity analysis for photovoltaic water pumping systems," *Sol. Energy*, vol. 144, pp. 376–391, Mar. 2017, doi: 10.1016/j.solener.2017.01.040.
[30] R. B. Ammar, M. B. Ammar, and A. Oualha, "Photovoltaic power forecast using empirical models and artificial intelligence approaches for water pumping systems," *Renew. Energy*, vol. 153, pp. 1016–1028, Jun. 2020, doi: 10.1016/j.renene.2020.02.065.
[31] M. Á. Pardo, J. Manzano, J. Valdes-Abellan, and R. Cobacho, "Standalone direct pumping photovoltaic system or energy storage in batteries for supplying irrigation networks. Cost analysis," *Sci. Total Environ.*, vol. 673, pp. 821–830, Jul. 2019, doi: 10.1016/j.scitotenv.2019.04.050.
[32] S. S. Kumar, C. Bibin, K. Akash, K. Aravindan, M. Kishore, and G. Magesh, "Solar powered water pumping systems for irrigation: A comprehensive review on developments and prospects towards a green energy approach," *Mater. Today, Proc.*, vol. 33, pp. 303–307, 2020, doi: 10.1016/j.matpr.2020.04.092.
[33] J. K. Kaldellis, G. C. Spyropoulos, K. A. Kavadias, and I. P. Koronaki, "Experimental validation of autonomous PV-based water pumping system optimum sizing," *Renew. Energy*, vol. 34, no. 4, pp. 1106–1113, Apr. 2009, doi: 10.1016/j.renene.2008.06.021.
[34] J. P. Paredes-Sánchez, E. Villicaña-Ortíz, and J. Xiberta-Bernat, "Solar water pumping system for water mining environmental control in a slate mine of Spain," *J. Cleaner Prod.*, vol. 87, pp. 501–504, Jan. 2015, doi: 10.1016/j.jclepro.2014.10.047.
[35] M. Das and R. Mandal, "A comparative performance analysis of direct, with battery, supercapacitor, and battery-supercapacitor enabled photovoltaic water pumping systems using centrifugal pump," *Sol. Energy*, vol. 171, pp. 302–309, Sep. 2018, doi: 10.1016/j.solener.2018.06.069.
[36] X. Fan, B. Liu, J. Liu, J. Ding, X. Han, Y. Deng, X. Lv, Y. Xie, B. Chen, W. Hu, and C. Zhong, "Battery technologies for grid-level large-scale electrical energy storage," *Trans. Tianjin Univ.*, vol. 26, no. 2, pp. 92–103, Apr. 2020, doi: 10.1007/s12209-019-00231-w.
[37] F. Nadeem, S. S. Hussain, P. K. Tiwari, A. K. Goswami, and T. S. Ustun, "Comparative review of energy storage systems, their roles, and impacts on future power systems," *IEEE Access*, vol. 7, pp. 4555–4585, 2018, doi: 10.1109/ACCESS.2018.2888497.
[38] T. Chen, Y. Jin, H. Lv, A. Yang, M. Liu, B. Chen, Y. Xie, and Q. Chen, "Applications of lithium-ion batteries in grid-scale energy storage systems," *Trans. Tianjin Univ.*, vol. 26, no. 3, pp. 208–217, Jun. 2020, doi: 10.1007/s12209-020-00236-w.
[39] C. She, Z. Wang, F. Sun, P. Liu, and L. Zhang, "Battery aging assessment for real-world electric buses based on incremental capacity analysis and radial basis function neural network," *IEEE Trans. Transport. Electrific.*, vol. 16, no. 5, pp. 3345–3354, May 2020, doi: 10.1109/TII.2019.2951843.
[40] Q. Wang, Z. Wang, L. Zhang, P. Liu, and Z. Zhang, "A novel consistency evaluation method for series-connected battery systems based on real-world operation data," *IEEE Trans. Transport. Electrific.*, vol. 7, no. 2, pp. 437–451, Jun. 2021, doi: 10.1109/tte.2020.3018143.

[41] I. Mathews, B. Xu, W. He, V. Barreto, T. Buonassisi, and I. M. Peters, "Technoeconomic model of second-life batteries for utility-scale solar considering calendar and cycle aging," *Appl. Energy*, vol. 269, pp. 1–9, Jul. 2020, doi: 10.1016/j.apenergy.2020.115127.
[42] F. J. Gimeno-Sales, S. Orts-Grau, A. Escribá-Aparisi, P. González-Altozano, I. Balbastre-Peralta, C. I. Martínez-Márquez, M. Gasque, and S. Seguí-Chilet, "PV monitoring system for a water pumping scheme with a lithium-ion battery using free open-source software and IoT technologies," *Sustainability*, vol. 12, no. 24, pp. 1–28, Dec. 2020, doi: 10.3390/su122410651.
[43] United Nations—Dept. of Economic and Social Affairs. (2015). *Sustainable Development Goals*. Accessed: Feb. 23, 2020. [Online]. Available: https://sustainabledevelopment.un.org/sdgs
[44] J. Figgener, P. Stenzel, K.-P. Kairies, J. Linßen, D. Haberschusz, O. Wessels, G. Angenendt, M. Robinius, D. Stolten, and D. U. Sauer, "The development of stationary battery storage systems in Germany—A market review," *J. Energy Storage*, vol. 29, pp. 1–20, Jun. 2020, doi: 10.1016/j.est.2019.101153.
[45] K.-P. Kairies, J. Figgener, D. Haberschusz, O. Wessels, B. Tepe, and D. U. Sauer, "Market and technology development of PV home storage systems in Germany," *J. Energy Storage*, vol. 23, pp. 416–424, Jun. 2019, doi: 10.1016/j.est.2019.02.023.
[46] G. J. May, A. Davidson, and B. Monahov, "Lead batteries for utility energy storage: A review," *J. Energy Storage*, vol. 15, pp. 145–157, Feb. 2018, doi: 10.1016/j.est.2017.11.008.
[47] J. Timpert, "Application note battery energy storage systems: Efficiency and lifetime," Eur. Copper Inst., Brussels, Belgium, Tech. Rep. Cu0240, 2017.
[48] *Trends 2016 in Photovoltaic Applications: Survey Report of Selected IEA Countries Between 1992 and 2015*, IEA PVPS, Paris, France, 2016.
[49] *Solar Irrigation With Electric Vehicle: Public-Private Approach to Energy, Water and Food Nexus*, World Bank Group, Washington, DC, USA, 2014. [Online]. Available: https://documents.worldbank.org/en/publication/documents-reports/documentdetail/825921468142177741/solar-irrigation-with-electric-vehicle-public-private-approach-to-energy-water-and-food-nexus
[50] S. Anuphappharadorn, S. Sukchai, C. Sirisamphanwong, and N. Ketjoy, "Comparison the economic analysis of the battery between lithium-ion and lead-acid in PV stand-alone application," *Energy Procedia*, vol. 56, pp. 352–358, 2014, doi: 10.1016/j.egypro.2014.07.167.
[51] D. L. Wood, J. Li, and C. Daniel, "Prospects for reducing the processing cost of lithium ion batteries," *J. Power Sources*, vol. 275, pp. 234–242, Feb. 2015, doi: 10.1016/j.jpowsour.2014.11.019.
[52] M. Gasque, P. González-Altozano, R. P. Gutiérrez-Colomer, and E. García-Marí, "Optimisation of the distribution of power from a photovoltaic generator between two pumps working in parallel," *Sol. Energy*, vol. 198, pp. 324–334, Mar. 2020, doi: 10.1016/j.solener.2020.01.013.

S. ORTS-GRAU was born in Valencia, Spain, in 1972. He received the M.S. and Ph.D. degrees in electronic engineering from the Universitat Politècnica de València (UPV), Valencia, in 2000 and 2008, respectively. Since 2001, he has been lecturing with the Department of Electronics Engineering (UPV). He is involved in various research projects in the fields of advanced control of power electronics converters, control and efficiency improvement of renewable energy generation systems, and power quality optimization with active power converters.

P. GONZÁLEZ-ALTOZANO was born in Spain, in 1968. He received the M.S. and Ph.D. degrees in agricultural and food engineering from the Universitat Politècnica de València (UPV), Spain, in 1992 and 1998, respectively. He was a Predoctoral Fellow with the Instituto Valenciano de Investigaciones Agrarias (IVIA), from 1994 to 1998, where he held a postdoctoral contract, from 1998 to 1999. Since 2001, he has been a Lecturer with the Department of Rural and Agrifood Engineering, UPV. His current research interests include is marked by his involvement in research and development projects, as well as his scientific publications include: solar energy systems, photovoltaic pumping systems, thermal energy storage, irrigation water management, and water saving.

FRANCISCO J. GIMENO-SALES was born Valencia, Spain, in 1958. He received the Ph.D. degree in electronic engineering from UPV, in 2004. From 1986 to 1993, he worked in several research and development departments developing industrial products (hardware and software). Since 1993, he has been teaching power electronics and digital control applied to power converter control at EED-UPV. His research interests include intelligent control of power electronics converters and the IoT intelligent communications systems applied to machine learning.

I. BALBASTRE-PERALTA was born in Spain, in 1972. He received the M.S. and Ph.D. degrees in agricultural and food engineering from the Universitat Politècnica de València (UPV), Spain, in 1998 and 2016, respectively. He was a Predoctoral Fellow at UPV, from 1998 to 2000, where he has been a Lecturer with the Department of Rural and Agrifood Engineering, since 1999. He has been the Head of Hydraulic Engineering Laboratory (LHIR-UPV), since 2008. His current research interests include is marked by his involvement in research and development projects as well as his scientific publications are the characterization of hydraulic elements, design of pressure irrigation systems, GIS, solar energy systems, photovoltaic pumping systems, irrigation water management, and precision irrigation.

C. I. MARTÍNEZ MÁRQUEZ was born in Xalapa, Mexico, in 1987. He received the M.E. degree in electronic systems engineering and the Ph.D. degree in electronic engineering from the Universitat Politècnica de València (UPV), Spain. He is currently a Researcher with the Department of Electronic Engineering, UPV. His main research interests include renewable energy systems, digitally controlled power converters, and embedded systems.

M. GASQUE was born in Valencia, Spain, in 1968. She received the M.S. and Ph.D. degrees in agricultural and food engineering from the Universitat Politècnica de València (UPV), Valencia, Spain, in 1992 and 1999, respectively. She was a Predoctoral Fellow with the Desertification Research Center (CIDE-CSIC), Valencia, from 1995 to 1999. She was a Postdoctoral Fellow with the School of Technology and Experimental Sciences, Universitat Jaume I, Castellon, Spain, from 1999 to 2000, and the Institute of Agrochemistry and Food Technology (IATA-CSIC), Valencia, in 2001. Since 2001, she has been a Lecturer with the Department of Applied Physics, UPV. Her current research interests include is marked by her involvement in research and development projects, as well as her scientific publications in international journals specialized in various areas, include: energy optimization, photovoltaic pumping systems, thermal energy storage, water saving, and irrigation water management.

S. SEGUI-CHILET was born in Valencia, Spain, in 1962. He received the B.E. degree in industrial electronics from UPV, in 1986, the M.E. degree in electronic engineering with the Universitat de València (UV), in 1999, and the Ph.D. degree in electronics engineering from UPV, in 2004. Since 1990, he has been a Lecturer with the Department of Electronic Engineering, UPV. Since 2006, he has been led various face-to-face and on-line postgraduate courses on photovoltaics. His major research interests include power electronics, renewable energy systems, and active power compensators.